

Probable member stars of the gravitational theory-testing globular clusters AM 1, Pal 3 and Pal 14^{*}

Michael Hilker¹

Sternwarte der Universität Bonn, Auf dem Hügel 71, 53121 Bonn, Germany

Received 10 October 2005 / Accepted 17 October 2005

Abstract. Some of the Galactic outer halo globular clusters are excellent tools to probe gravitational theories in the regime of weak accelerations (Baumgardt et al. 2005). The measurement of the line-of-sight velocity dispersion among stars in these clusters will differentiate between the validity of Newtonian dynamics (low velocity dispersion) and the possibility of modified Newtonian dynamics (MOND) or dark matter dominated globular clusters (high velocity dispersion). In this paper, the properties of probable member stars of the three best-case gravitational theory-testing clusters AM 1, Pal 3 and Pal 14 are presented. The member selection is based on VLT photometry in Johnson *BV*. The positions of the stars were determined with an accuracy of the order $\leq 0''.2$, allowing their direct use for follow-up spectroscopy. The distance, reddening, age, and metallicities of the clusters were estimated from isochrone fitting. Furthermore, improved structural parameters, like central coordinates, ellipticity, half-light radius, King model core and tidal radius, are presented.

Key words. globular clusters: individual: AM 1, Pal 3, Pal 14
– astrometry — galaxy: kinematics and dynamics

1. Introduction

In the distant halo of our Milky Way there exist several low mass, often diffuse globular clusters (GCs). Most of these outer halo GCs belong to the so-called ‘young halo clusters’, comprising about 30 Milky Way GCs (e.g. Zinn 1993, Mackey & Gilmore 2004). From their horizontal branch morphology it was estimated that they are about 1-2 Gyr younger than the ‘old halo clusters’. Also they have on average larger half-light radii than the inner halo GCs (Mackey & van den Bergh 2005). The similarity of their properties to those of external globular clusters (belonging to Milky Way satellite galaxies) led to the idea that they were accreted into the Galactic halo (e.g. van den Bergh & Mackey 2004, originally proposed by Searle & Zinn 1978). The most remote halo GCs (at galacto-centric distances of ≥ 100 kpc) live on eccentric orbits, mostly undisturbed from external tidal forces of our Galaxy.

Recently, it has been proposed by Baumgardt et al. (2005) that some of these distant Galactic globular clusters are excellent tools to probe gravitational theories in the regime of very weak accelerations. Their internal and external accelerations both are significantly below the critical acceleration parameter a_0 of modified Newtonian dynamics (MOND, Milgrom 1983,

Bekenstein & Milgrom 1984). In case of MOND the internal velocity dispersion among the stars in these clusters would be significantly higher than in the Newtonian standard dynamics. A higher than Newtonian velocity dispersion could also be explained by the existence of dark matter in globular clusters (e.g. Mashchenko & Sills 2005). The line-of-sight velocity dispersion of the 8 gravitational theory-testing GCs listed by Baumgardt et al. (2005) is expected to range between 0.5 and 1.1 km²/sec² in the Newtonian case, whereas two times higher values (1.1 to 2.4 km²/sec²) are predicted for MOND. Such velocity differences can be measured with existing high resolution spectrographs, providing the observation of a statistical meaningful sample (~ 20 -30) of stars.

However, at the distance of the proposed GCs of between 28 and 122 kpc, high resolution spectroscopic observations of these feeble, low mass clusters are challenging. There exist only few evolved stars that are bright enough to be observed in reasonable integration times with 8-meter class telescopes. Therefore, it is very useful to know the positions and photometric properties of these bright member stars beforehand.

For three of the Baumgardt-sample GCs we present those properties in this paper, namely AM 1, Pal 3 and Pal 14. These clusters were selected because they are expected to show the largest differences between Newtonian and MOND dynamics. They are therefore the best cases for testing gravitational theories. Their basic parameters are given in the Tables 3 and 4 (most of these parameters were taken from the 2003 version of Harris’ list 1996). All three clusters belong to the ‘young halo’ GCs with iron abundances between -1.5 and -1.8 dex, and half-light radii in the range 17-25 pc. An age estimate for Pal 3 was derived from the detailed study of the colour magnitude

Send offprint requests to: M. Hilker

^{*} Based on observations obtained at the European Southern Observatory, Chile (Observing Programme 074.D-0187).

Correspondence to: mhilker@astro.uni-bonn.de

Table 1. Observation log. The appendices ‘N’ and ‘S’ in the GC names denote the pointings North and South of their centers, respectively.

Name	$\alpha(2000)^a$ [h:m:s]	$\delta(2000)^a$ [°:′:″]	Date	Exposure times [s]		Seeing [″]		Airmass	
				<i>B</i>	<i>V</i>	<i>B</i>	<i>V</i>	<i>B</i>	<i>V</i>
AM 1-N	03:55:02.6	−49:34:41.9	2005 Feb 15	3 × 25	3 × 10	0.6	0.7	1.20	1.20
AM 1-S	03:55:02.6	−49:38:42.0	2005 Feb 16	3 × 30	3 × 15	0.6	0.6	1.21	1.22
Pal 3-N	10:05:31.4	+00:06:25.9	2005 Feb 15	3 × 25	3 × 10	0.6	0.7	1.24	1.23
Pal 3-S	10:05:31.4	+00:02:26.0	2005 Feb 15	3 × 25	3 × 10	0.5	0.5	1.22	1.21
Pal 14-N	16:11:05.0	+14:59:38.0	2005 Feb 15	3 × 25	3 × 10	0.6	0.7	1.46	1.45
Pal 14-S	16:11:05.0	+14:55:37.9	2005 Feb 15	3 × 25	3 × 10	0.5	0.6	1.43	1.42

^aThe coordinates indicate the pointing of the observations

Table 2. Calibration coefficients for both nights. The zero points apply for magnitudes transformed from intensities in counts/sec. The signs are such that the following calibration equation applies: $mag_{cal} = mag_{inst} + ZP + k \times AM + CT \times (B - V)_{cal}$, with ZP = zero point, k = extinction coefficient, AM = airmass, and CT = colour term.

Chip	Filter	zero point	ext. coeff.	colour term
chip1	<i>V</i>	27.852±0.002	−0.123±0.011	0.034±0.008
	<i>B</i>	27.295±0.009	−0.185±0.016	−0.031±0.006
chip2	<i>V</i>	27.841±0.012	−0.162±0.018	0.020±0.004
	<i>B</i>	27.298±0.008	−0.208±0.016	−0.033±0.006

diagram, especially the horizontal branch (HB) morphology. It seems that Pal 3 is between 1 Gyr (VandenBerg 2000, Catelan et al. 2001) and 2 Gyr (Stetson et al. 1999) younger than ordinary inner halo GCs like M3. Also for Pal 14 a 3 to 4 Gyr younger age than for typical GCs was estimated from the position of the main sequence turnoff (MSTO) relative to the HB level (Sarajedini 1997).

In this paper, we provide accurate positions, V magnitudes and $(B - V)$ colours of the evolved stars in the three clusters AM 1, Pal 3 and Pal 14. This photometry is necessary and very useful for spectroscopic follow-up observations of these best-case gravitational theory-testing clusters.

2. Observations and data reduction

The observations were performed in February 2005 with the VLT/UT1 at Paranal (ESO), Chile. The instrument in use was the FORS2 camera with a 4×4 k MIT CCD array attached. The data were read out with a 2×2 binning, resulting in a spatial scale of $0.25''/\text{pixel}$ and a field of view of $6'.8 \times 6'.8$.

Each of the three globular clusters AM 1, Pal 3 and Pal 14 was observed through the Johnson B and V filters under mostly photometric and very good seeing conditions at two slightly different positions. Once, centering the cluster on the ‘master’ 4×2 k chip (also called “chip1”), and once on the ‘slave’ 4×2 k chip (=“chip2”) of the 1×2 CCD array. Excerpts of the V exposures on the ‘master’ chip are shown in Fig. 1. The exposure times were chosen such that the brightest cluster red giants were not saturated. Three dithered integrations per filter and field were taken. For an observation log see Table 1.

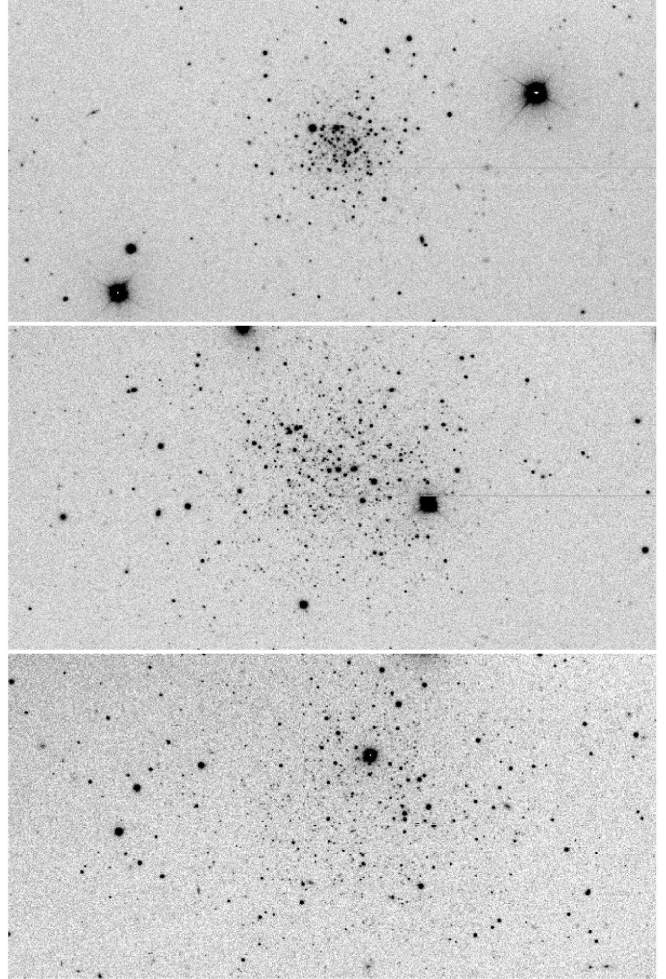


Fig. 1. Excerpts of the combined V images for AM 1 (top), Pal 3 (middle) and Pal 14 (bottom). $4' \times 2'$ sections of the corresponding ‘master’ chips are shown. North is up, East is left.

The CCD frames were processed with standard IRAF routines. After bias subtraction and flatfield correction, the pixel shifts of the dithered images have been determined. Then the shift corrected frames have been averaged using a clipping algorithm to exclude cosmics.

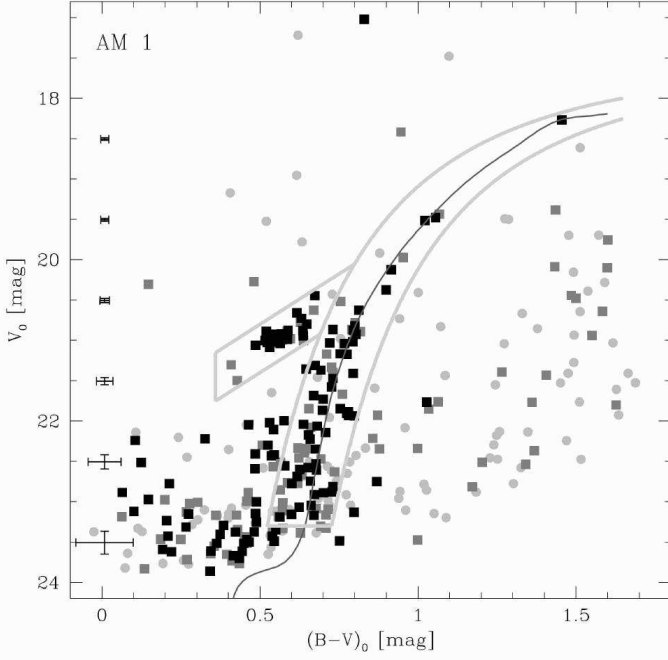


Fig. 2. Colour magnitude diagram of stars around AM 1. The reddening is negligible: $E_{B-V} = 0.0$ mag. Dark grey squares are those objects that are located within five half-light radii from the centre of the cluster, black squares those within one half-light radius (see Fig. 3). Typical photometric errors are shown on the left. The selection areas for probable member stars are marked (red giant branch and horizontal branch). Overplotted is a Yonsei-Yale isochrone (Kim et al. 2002) with the following parameters: age = 11 Gyr, $[\text{Fe}/\text{H}] = -1.4$ dex, $[\alpha/\text{Fe}] = 0.3$ dex. The isochrone has been shifted with $(m - M)_{V,0} = 20.45$ mag and $(B - V)_{\text{corr.}} = -0.01$ mag (see text for further details).

3. Photometry and astrometry

3.1. Photometry

The instrumental magnitudes of the stars were derived from PSF (point spread function) photometry using DAOPHOT II (Stetson 1987, 1992). For the comparison with the standard stars, aperture-PSF shifts have been determined in all fields and filters. The amplitude of this shift ranges between 0.20 and 0.44 mag, its uncertainty is of the order of 0.02 mag.

In the first night, Landolt standard stars have been observed. The coefficients of the calibration equation were taken from the ESO quality control program (see <http://www.eso.org/observing/dfo/quality/index.fors2.html>). An overview of the calibration coefficients is given in Table 2.

The calibrated magnitudes of stars in the overlapping regions of the North and South fields have been compared with each other. Shifts of the order of ± 0.02 mag have been found between the data sets. This is consistent with the uncertainty in the aperture-PSF shift, but could also have been caused by the not totally photometric conditions during the observing run. Thus, the data set which was observed under better photometric conditions has been taken as reference system for each cluster,

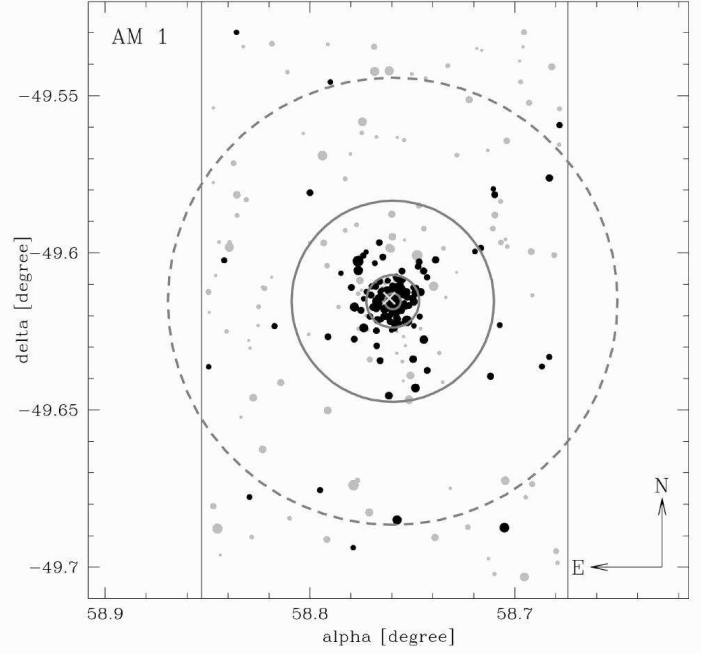


Fig. 3. Coordinates of stars around AM 1. The symbol size corresponds to the luminosity of an objects: the larger the dot the brighter the star. Black dots are probable member stars according to their position in the CMD (see highlighted areas in Fig. 2). The solid circles are from inside out the core radius, the half-light radius and the tidal radius (Harris 1996). The dashed circle is the tidal radius as calculated by Baumgardt et al. (2005). All circles are centred on the newly determined central coordinates of AM 1 (see Table 3). The cross marks the central coordinate from the list of Harris (Harris 1996). The vertical lines indicate the borders of our field-of-view.

and the magnitudes of the other set have been shifted to this system. The magnitudes of stars that were measured in both data sets then have been averaged for the final catalog.

After the photometric reduction, calibration of the magnitudes, and combining of the data sets, the average photometric errors for red giants at $V = 23$ were of the order of 0.08 in V and 0.12 mag in B .

3.2. Astrometry

The positions of the cluster stars in terms of right ascension and declination (epoch J2000) were determined by deriving an astrometric solution between pixel and RA/Dec coordinates for stars of the US Naval Observatory (USNO) in the field-of-view. Each CCD chip has been considered separately. Typically, between 60 and 80 USNO catalog stars were identified in chip1, and 40-60 in chip2. The IRAF task GEOMAP was used to find the astrometric solution. A ‘general’ fit with full cross-terms of second order turned out to give the best results. The rms of the fit in right ascension is $0''.17$ for AM 1 and Pal 14, and $0''.24$ for Pal 3. The accuracy in declination is $0''.14$, $0''.17$, and $0''.19$ for AM 1, Pal 14, and Pal 3, respectively.

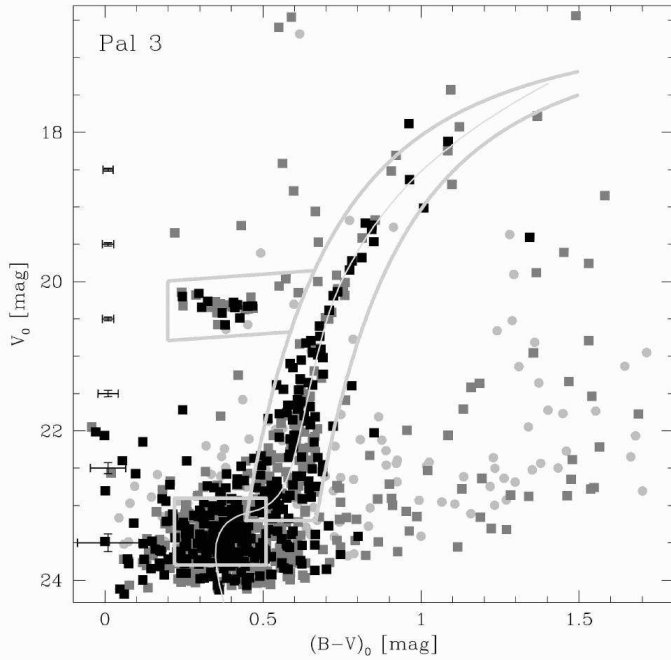


Fig. 4. Reddening corrected CMD of stars around Pal 3 ($E_{B-V} = 0.040$ and $A_V = 0.124$ mag). Symbols and areas as in Fig. 2. Additionally, the area of main sequence turnoff stars is marked. The isochrone parameters are: age = 10 Gyr, $[\text{Fe}/\text{H}] = -1.7$ dex, $[\alpha/\text{Fe}] = 0.3$ dex, $(m - M)_{V,0} = 19.95$ mag, and $(B - V)_{\text{corr.}} = -0.02$ mag.

The coordinates of the member stars are listed in the Tables A.1, A.2, and A.3. The derived coordinates also were used for the graphs of Figs. 3, 5, and 7.

4. Distance, reddening, age and metallicity

The calibrated and de-reddened magnitudes are presented in the colour-magnitude diagrams (CMDs, see Figs. 2, 4, and 6). The foreground reddening has been corrected with the E_{B-V} values given in the Harris list (Harris 1996), and $A_V = 3.1E_{B-V}$. Only stars with photometric errors less than 0.15 mag in V and B and ALLSTAR *sharp* and *chi* values in the ranges $-0.7 < \text{sharp} < 1.0$ and $\text{chi} < 3.0$ are shown. The red giant branch (RGB) and horizontal branch (HB) are clearly visible in all clusters. For Pal 3, even the main sequence turnoff (MSTO) region is well defined.

The distances to the clusters are derived from the apparent magnitude of the horizontal branch. We selected only those HB stars which are located within five half-light radii from the clusters' centres and which lie on the horizontal part of the HB at $(B - V)_0 \sim 0.5$ (to avoid AGB and extended HB stars). The average HB magnitudes in V and the corresponding distance moduli are given in Table 3. They agree within ± 0.03 mag with the values listed by Harris (1996).

In order to estimate the age and metallicity of the clusters we fitted the location and shape of the RGBs by appropriate isochrones. The Yonsei-Yale isochrone set by Kim et al. (2002) was used for that. An alpha-abundance of $[\alpha/\text{Fe}] = 0.3$ dex was

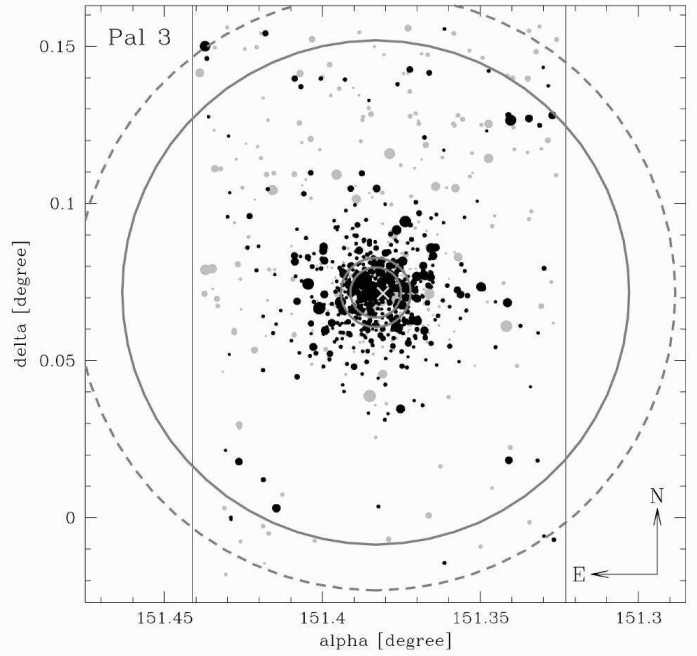


Fig. 5. Coordinates of stars around Pal 3. For the explication of symbols, see Fig. 3.

adopted. The best-fitting isochrones are shown in Figs. 2, 4, and 6. They have ages between 10 and 11 Gyr, and metallicities in the range -1.7 to -1.4 dex. For Pal 3 and Pal 14 the best-fitting metallicity value agrees well with the spectroscopic values in the Harris list (see Table 3). For AM 1, no good isochrone fit with a metallicity of -1.8 dex could be found. Instead, a metallicity of -1.4 dex represents the shape of the RGB well. Either, the spectroscopic abundance is not accurate enough and this cluster indeed has a higher metallicity or, the isochrone fit is not constrained well enough. Besides the selection of the best-fitting ages and metallicities, the isochrones had to be slightly shifted in V as well as in $(B - V)$ to match the exact location of the RGB. These corrections are given in the captions of the CMD figures, $(m - M)_{V,0}$ and $(B - V)_{\text{corr.}}$, and in Table 3 (with $E_{B-V, \text{this work}} = E_{B-V, \text{Harris}} + (B - V)_{\text{corr.}}$). These corrections are of the order of the photometric errors and within the uncertainties of not perfectly photometric conditions.

4.1. Member selection

The main purpose of this paper is to provide a list of bright cluster members for follow-up spectroscopy. Therefore, probable cluster members have to be selected. The principle criterium is that member stars should be located close to the isochrone in the colour-magnitude diagram. A second criterium is their distance to the cluster centre. In the Figs. 2, 4, and 6 the regions of probable member stars are high-lighted. The RGB and HB regions are marked for all clusters. In Pal 14, an additional region of subgiant branch (SGB) stars has been selected, in Pal 3 also the MSTO region. Furthermore, stars within one and five half-light radii are shown in the graphs as black and dark grey squares, respectively. The core radius, half-light ra-

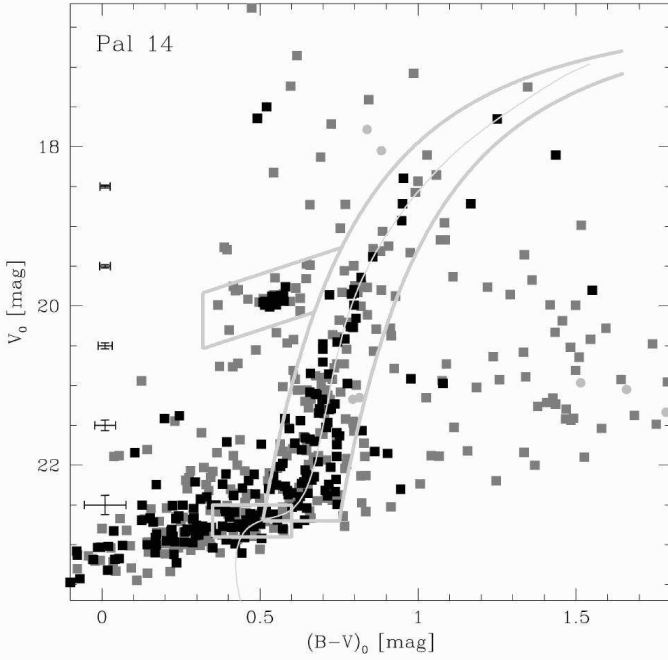


Fig. 6. Reddening corrected CMD of stars around Pal 14 ($E_{B-V} = 0.040$ and $A_V = 0.124$ mag). Symbols and areas as in Fig. 2. The lowest area includes probable subgiant branch stars. The isochrone parameters are: age = 10 Gyr, $[\text{Fe}/\text{H}] = -1.5$ dex, $[\alpha/\text{Fe}] = 0.3$ dex, $(m - M)_{V,0} = 19.42$ mag, and $(B - V)_{\text{corr.}} = 0.03$ mag.

dus and tidal radius (Harris 1996, Baumgardt et al. 2005) are listed in Table 4 and shown in Figs. 3, 5, and 7.

In the Appendix, magnitude limited samples of probable member stars are listed (Tables A.1, A.2, and A.3). Only stars within the tidal radius given by Baumgardt et al. (2005) have been considered. The magnitude limits are $V_0 = 23.0$, 22.5, and 22.2 for AM 1, Pal 3, and Pal 14, respectively. Thus, only RGB, HB and AGB stars are contained in the lists. Note: the full tables only are available in the online version of the article.

5. Structural parameters

Although the photometry of the observed clusters is not very deep and we do not sample the main sequence stars, some structural parameters of the globular clusters can be derived from the selected evolved member stars.

5.1. Cluster centres

The cluster centres were determined by analysing the number distribution of probable member stars as function of right ascension and declination. Probable member stars are those of the high-lighted regions in the CMDs (see Figs. 2, 4, and 6). Furthermore, the member stars have been restricted to an approximately squared region ($6.5' \times 6.5'$) around their apparent cluster centres. The number distributions of the stars are shown in Fig. 8 as histograms and as binning independent representations (using an Epanechnikov kernel). The binning indepen-

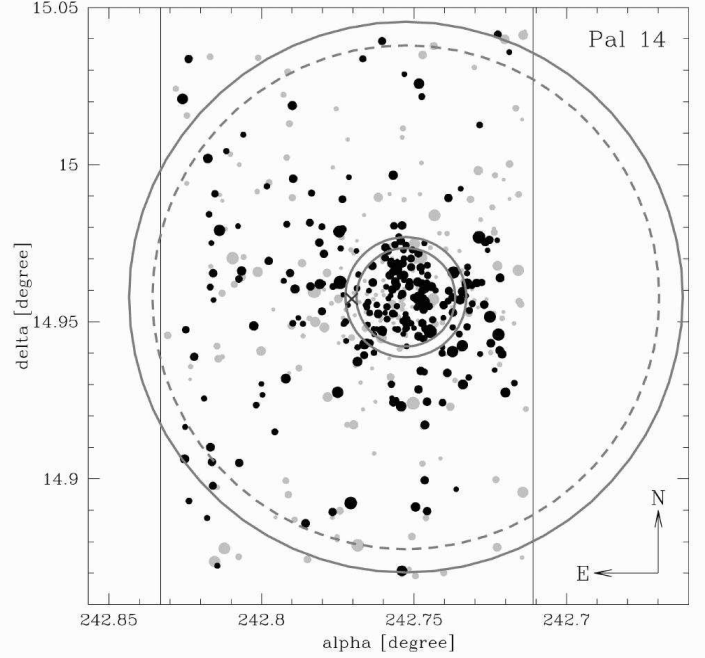


Fig. 7. Coordinates of stars around Pal 14. For the explication of symbols, see Fig. 3.

dent number distributions were fitted by Gaussians. The peak of these Gaussians defines the cluster centre. In Table 3 the derived values are listed. The accuracy of the centre determination is about $\pm 2''$. Whereas the declination of the centres agree very well with those listed in the Harris list, there are some notable deviations in the right ascension (see also crosses in Figs. 3, 5, and 7). Especially, the right ascension listed for Pal 14 is off by $\sim 62''$ with respect to our value. We are confident that our values are very accurate and suggest to correct the coordinates in the ‘official’ lists (e.g. Harris 1996).

5.2. Angular distribution and ellipticity

The ellipticity of the clusters is of interest because rotation or the tidal loss of stars in opposite directions might cause a detectable signal. To investigate this we studied the angular distribution of probable member stars including the main sequence turnoff region stars (see Fig. 9). We choose the radial range to be from outside the core radius (only for AM 1 and Pal 3) to avoid crowding effects to inside the maximum radius of the observed CCD area to guarantee a homogeneous angular coverage. The angular distributions (counted in bins of 20 degree) then were fitted by a double-cosine function of the form $N = A + B \cdot \cos(2 \cdot (\phi + C))$, where A and B define the ellipticity as follows: $\epsilon = (A - B)/(A + B)$, assuming that the ellipticity is expressed as $1 - b/a$ (a : semi major axis, b : semi minor axis). The error for the ellipticity was propagated from the Poisson statistics of the number counts and the rms of the fit. The results are: $\epsilon_{\text{AM 1}} = 0.20 \pm 0.26$, $\epsilon_{\text{Pal 3}} = 0.11 \pm 0.20$, and $\epsilon_{\text{Pal 14}} = 0.13 \pm 0.10$. None of the clusters exhibits a significant ellipticity. The distribution of their stars is compatible with a homogeneous, circular distribution within the errors.

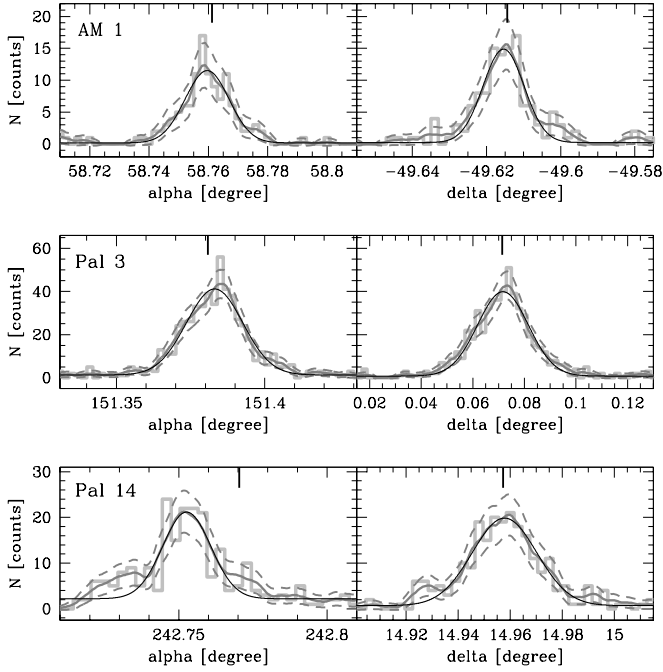


Fig. 8. Determination of globular cluster centres from the spatial distribution of selected probable member stars (see the CMDs). The grey histograms in the left panels show the distribution in West-East-direction, the ones in the right panels the distribution in South-North-direction. Binning independent representations of the counts (Epanechnikov kernel of 0.002 (AM 1 and Pal 3) and 0.003 (Pal 14) degree width) are overplotted as thin curves, together with their 1σ uncertainty limits (dashed curves). The thick-lined Gaussians are fits to the binning independent distributions. The bold tickmarks on top of each plot mark the central positions from the Harris catalog (1996).

5.3. Surface density profiles

The probable member stars of the three clusters are evolved stars of more or less the same mass. Since they are the brightest stars of the clusters they dominate the surface brightness of those clusters. One can derive the structural parameters of the clusters by fitting density profiles to either the number density distribution or the surface brightness distribution of the stars. This is shown in Fig. 10. The number density counts have been corrected for background/foreground field star contamination by estimating the field star number counts from 0.5 arcmin wide strips in the northern and southern edge of the observed CCD areas. The number density of contaminating field stars in the selected CMD areas is 0.15, 0.77, and 0.62 objects/arcmin⁻² for AM 1, Pal 3, and Pal 14, respectively. The core radius, the tidal radius, and the central surface brightness of the clusters were determined from the best fitting King (King 1962) profiles. For Pal 14, the tidal radius had to be fixed to 5 arcmin (the mean value between Harris 1996 and Baumgardt et al. 2005) since it could not be constrained by the fit. The half-light radii were derived from a curve-of-growth analysis of the integrated light of the member stars. The results of our analyses are given in Table 4. Typical errors are of the order 0'06 (AM 1,

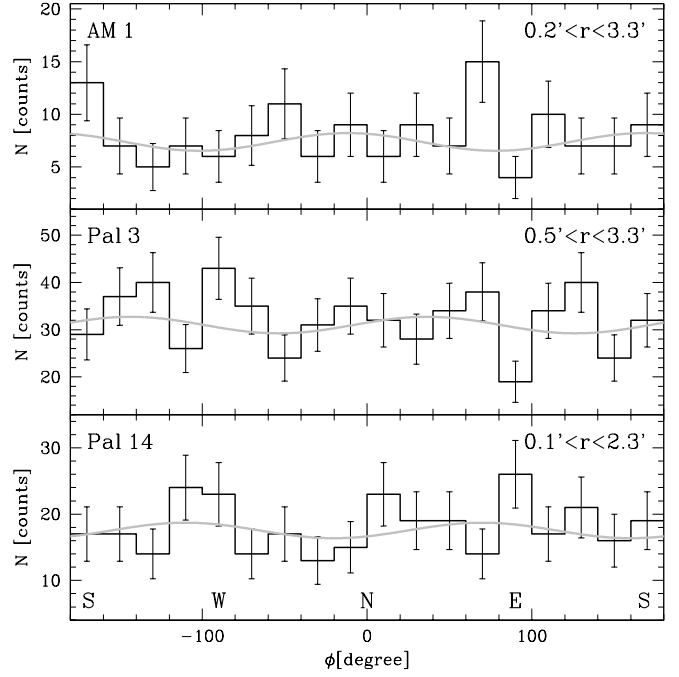


Fig. 9. The angular distribution of probable member stars in the indicated radial ranges around the three clusters is shown together with statistical errorbars. The grey curves are best-fitting double-cosines, indicating the ellipticity of the clusters.

Pal 3) and 0'20 (Pal 14) for r_c , 0'04 (Pal 3) and 0'19 (AM 1) for r_t , while for r_h they are $\sim 0'02$ respectively. The errors for the central surface brightness are between 0.25 and 0.40 mag.

Not all our derived values agree with the ones listed by Harris (1996) and/or Baumgardt et al. (2005). For AM 1, we find a slightly smaller half-light radius, but a significantly larger tidal radius than listed by Harris. A small tidal radius does not fit the profile. Also the central surface brightness is much higher than Harris' value. In the contrary, for Pal 3, we derive a slightly larger half-light radius, but a smaller tidal radius. Also for Pal 14, a larger half-light radius fits the profile best.

Note however that all our values are valid for the selected probable member stars. Adding the fainter, lower mass main sequence stars would raise the central surface brightness a little bit. One might think that including the faint stars would increase the characteristic radii since these stars might be more widely distributed than the more massive, evolved stars due to the dynamical evolution of the cluster. However, the half-mass relaxation times of the clusters are between 5.5 and 9.1 Gyr, close to a Hubble time. This suggests that dynamical evolution does not play a major role in the shaping of the clusters.

6. Discussion and Summary

The outer halo globular clusters AM 1, Pal 3, and Pal 14 were imaged with FORS2 on the VLT under good seeing and mostly photometric conditions. Accurate PSF photometry in Johnson *BV* of stars brighter than $V = 24$ mag was performed in $6'8 \times 10'8$ large fields around these clusters. The absolute position of the stars was determined with an accuracy of $< 0.2''$

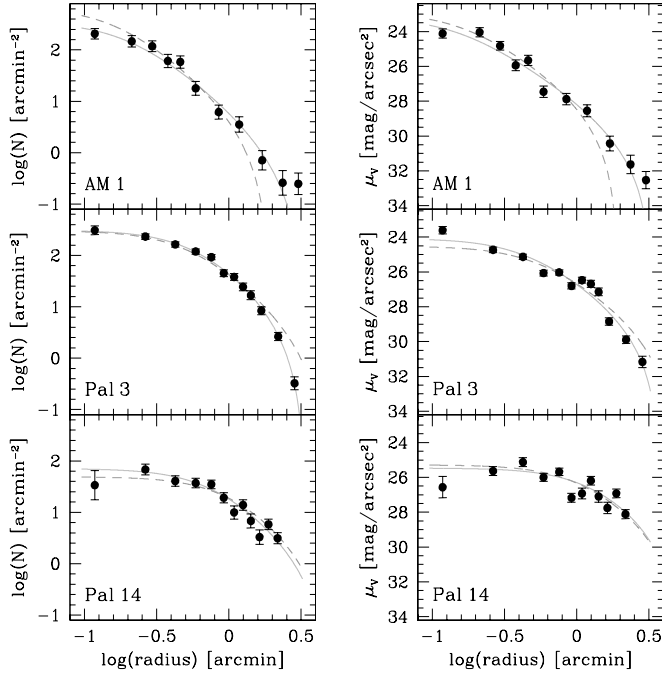


Fig. 10. The surface number density distribution (left panels) and the surface brightness distribution (right panels) of probable member stars is shown for the three clusters. The grey curves are best-fitting King models. Dashed curves are fits to the distributions when adopting the values for r_c and r_t of Harris' list (1996). The parameters of both fits are given in Table 4.

by applying a general astrometric solution derived from stars of the USNO catalog in the observed fields. This positional accuracy is sufficient to be used in input catalogs for most of the available multi-object spectrographs (using either fibres or slit masks).

Probable member stars of the clusters were selected according to their position in the colour-magnitude diagram and their distance to the cluster centres. The positions and photometric properties (V magnitude, $(B-V)$ colour) of all probable member stars within the tidal radius (as calculated by Baumgardt et al. 2005) and brighter than $V_0 = 23.0, 22.5, 22.2$ mag for AM 1, Pal 3, and Pal 14, respectively, are presented in the tables of the appendix. Although challenging, one can reach with modern high resolution spectrographs, like UVES at the VLT, a signal-to-noise above 10 for stars as faint as $V = 20.5$ mag within one observing night. This limit would mean a sample size of 9, 48, and 72 probable member stars for AM 1, Pal 3, and Pal 14, respectively. Except for AM 1, these sample sizes are sufficient to derive an accurate radial velocity dispersion of the clusters.

The colour-magnitude diagrams have been used to estimate – by isochrone fitting – distances, reddenings, ages and metallicities to the three clusters. Our derived values for the horizontal branch magnitude V_{HB} , reddening and distance modulus $(m-M)_V$ generally agree within ± 0.03 mag with the values given in the literature (AM 1: Madore & Freedman 1989; Pal 3: Stetson et al. 1999; Pal 14: Holland & Harris 1992). Only

for Pal 14 we get a slightly better isochrone fit when adopting a 0.05 mag shorter distance modulus and a 0.03 mag higher reddening (see Table 3). Since the turnoff regions are not very well constrained in the CMDs of the three clusters, age estimates have to be taken with caution. However, we found that isochrones with ages of 10-11 Gyr fit the turnoff-SGB-RGB transition region better than those of older ages. Our age estimates are consistent with the idea that the three clusters belong to the 'young halo' GCs which are, on average, 1-2 Gyr younger than the old 'inner halo' GCs (e.g. Mackey & Gilmore 2004). The metallicity of the chosen isochrones is mainly constrained by the shape of the red giant branch. The adopted values for Pal 3 (-1.7 dex) and Pal 14 (-1.5 dex) agree well with those given in the literature: Pal 3: -1.78 (Zinn 1985), -1.57 ± 0.3 (Armandroff et al. 1992), -1.70 ± 0.15 (Ortolani & Gratton 1989); Pal 14: -1.47 ± 0.3 (Zinn 1985), -1.60 ± 0.18 (Armandroff et al. 1992). The isochrone of AM 1, however, fits the RGB better with a higher metallicity (-1.4 dex) than derived in previous work: -1.69 (Zinn 1985), -1.7 ± 0.2 (Suntzeff et al. 1985). New spectroscopic metallicities are needed to decide whether AM 1 really is more metal-rich than thought before.

From the spatial distribution of probable member stars in AM 1, Pal 3, and Pal 14 structural parameters of the clusters have been determined and compared to the values given in Harris' list (1996) and Baumgardt et al. (2005). Whereas the derived declinations of all clusters agree with the literature values within $\pm 3''$, the right ascensions show larger deviations: $4''$ for AM 1, $7''$ for Pal 3, and most significantly $62''$ for Pal 14. The deviating right ascension of Pal 14 goes back to the list of Webbink (1985), and then was taken over into the lists of Djorgovski & Meylan (1993) and Harris (1996).

Concerning ellipticities, none of the clusters shows a measurable signal. They all seem to be relaxed, roundish halo clusters. Note however that a wide field study of main sequence stars around Pal 3 revealed a weak signature of extra tidal member stars between one and four tidal radii (Sohn et al. 2003).

The half-light radii of the clusters were estimated from curve-of-growth analyses of the integrated light of the probable member stars. Our derived values deviate by $\pm 0.2'$ from those given in Harris' list which are based on CCD work by Trager et al. (1993) and van den Bergh et al. (1991). Biases in the different selection of member stars and the accidental inclusion of foreground stars might explain these differences. The core and tidal radii of the three clusters were derived from King profile fits to their surface number density as well as surface brightness profiles. For AM 1 and Pal 3 both radii could be determined with stable solutions. For Pal 14, the spatial extension of the member stars was not sufficient enough to get a stable fit for the tidal radius. It was fixed to $5'$, the mean value of Harris (1996) and Baumgardt et al. (2005). The core and tidal radius of Pal 14 in Harris' list is based on the photographic study by Harris & van den Bergh (1984), the ones of AM 1 and Pal 3 on the CCD work by Trager et al. (1993). The main differences of our findings to previous literature values are that AM 1 definitely has a larger tidal radius than claimed by Trager et al. (1993), but smaller than calculated by Baumgardt et al. (2005). On the contrary, the tidal radius of Pal 3 seems to be

Table 3. Basic photometric parameters of AM 1, Pal 3, and Pal 14. The second row for each cluster gives the values from Harris’ list (1996). $E_{B-V,S98}$ is the reddening value by Schlegel et al. (1998). The magnitude of the horizontal branch V_{HB} and the total apparent V magnitude V_{tot} are not corrected for extinction. The first distance modulus is based on the derivation of the absolute magnitude of the HB using $M_{V,HB} = 0.15[Fe/H] + 0.8$, the second one on the isochrone fitting. The distance to the Sun R_{Sun} was calculated from the first distance modulus after correction for extinction with $A_V = 3.1E_{B-V,S98}$.

Name	RA(2000) [h:m:s]	Dec(2000) [°:′:″]	$E_{B-V,S98}$ [mag]	E_{B-V} [mag]	V_{HB} [mag]	$(m-M)_{V,HB}$ [mag]	$(m-M)_{V,iso}$ [mag]	[Fe/H] [dex]	R_{Sun} [kpc]	V_{tot}^a [mag]	M_V [mag]
AM 1	03:55:02.3	−49:36:55	0.01	...	20.98	20.39	20.45	−1.40	118.0	15.84	−4.55
	03:55:02.7	−49:36:52	...	0.00	20.96	20.43	...	−1.80	121.9	15.72	−4.71
Pal 3	10:05:31.9	00:04:18	0.04	0.02	20.48	19.94	19.95	−1.70	91.9	14.91	−5.03
	10:05:31.4	00:04:17	...	0.04	20.51	19.96	...	−1.66	92.7	14.26	−5.70
Pal 14	16:11:00.6	14:57:28	0.03	0.07	20.03	19.46	19.42	−1.50	74.7	14.68	−4.78
	16:11:04.9	14:57:29	...	0.04	20.04	19.47	...	−1.52	73.9	14.74	−4.73

^a The total magnitude in the first row for each cluster is based on the integrated luminosity of probable member stars down to the magnitude limits of the individual data sets. It therefore excludes most of the bright foreground stars, but also the fainter main sequence stars.

Table 4. Basic structural parameters of AM 1, Pal 3, and Pal 14. The second row for each cluster gives the values from Harris’ list (1996). The last three columns are physical scales based on the distances in Table 3.

Name	$\mu_{V,central}$ [mag/arcsec ²]	r_c^a [′]	r_h [′]	r_t^a [′]	$c^{a,b}$	r_c [pc]	r_h [pc]	r_t [pc]
AM 1	23.11	0.18 (0.14)	0.32	3.24 (3.29)	1.26 (1.37)	6.2 (4.8)	11.0	111.3 (113.0)
	23.86	0.15	0.50	1.92 (4.27)	1.12	5.3	17.7	68.1 (151.6)
Pal 3	23.84	0.54 (0.40)	0.72	3.34 (3.72)	0.79 (0.97)	14.4 (10.7)	19.3	89.3 (99.5)
	23.08	0.48	0.66	4.81 (5.69)	1.00	12.9	17.8	129.8 (153.5)
Pal 14	24.92	0.70 (1.14)	1.28	[5.00] ^c	0.85 (0.59)	15.2 (24.8)	27.8	[108.7] ^c
	25.55	0.94	1.15	5.26 (4.81)	0.75	20.21	24.7	113.1 (103.4)

^a In brackets the values of the fit to the surface brightness profile are given (first row for each cluster). The tidal radii in brackets of the second row for each cluster are the values from Baumgardt et al. (2005)

^b concentration parameter: $c = \log(r_t/r_c)$

^c this value was not derived but adopted

smaller than claimed by the two authors. The core radii of all clusters agree more or less with those given in Harris’ list. The three clusters have in common that their central concentration parameter is around 1.0, very low in comparison with ordinary inner halo globular clusters.

This paper provides the basis for further investigations of evolved stars in AM 1, Pal 3, and Pal 14. Future follow-up spectroscopic observations of these cluster will be very exciting. The measurements of a low (Newtonian) velocity dispersion would mean that MOND in its present form is in severe trouble and that globular clusters do not possess dark matter. In contrast, a high velocity dispersion would either favour MOND or could be a hint to the existence of dark matter in globular clusters, a highly interesting hypothesis on its own right.

Acknowledgements. I wish to thank Holger Baumgardt and Klaas de Boer for very helpful comments, and the anonymous referee for useful suggestions which improved the paper. This project was supported by the DFG project HI 855/2.

Appendix A: Lists of probable member stars

The following tables contain the lists of probable member stars of AM 1, Pal 3, and Pal 14. They are ordered with increasing V

magnitude. The columns are as follows:

Column 1. Identification number of the object, following the order of increasing V magnitude.

Column 2. Right ascension for the epoch 2000 in hours, minutes and seconds (^h, ^m, ^s).

Column 3. Declination (2000) in degrees, minutes and seconds (° , ′ , ″).

The positions of all objects were determined relative to positions in the USNO catalog. The positional accuracy of the calculated coordinates is in all fields better than 0.2″.

Column 4. V apparent magnitude as determined by PSF photometry under DAOPHOT II.

Column 5. $B - V$ colours from PSF photometry.

Column 6. Photometric error in V (ALLSTAR output).

Column 7. Photometric error in B (ALLSTAR output).

Column 8. Projected distance to cluster centre (see Table 3) in arcminutes.

Column 9. ‘Type’ describes to which part of the CMD the star probably belongs: RGB = red giant branch, HB = horizontal branch, AGB = asymptotic giant branch.

References

Armandroff, T. E., Da Costa, G. S., & Zinn, R. 1992, AJ, 104, 164

Baumgardt, H., Grebel, E. K., & Kroupa, P. 2005, MNRAS, 359, L1
 Bekenstein, J., & Milgrom, M. 1984, ApJ, 286, 7
 Catelan, M., Ferraro, F. R., & Rood, R. T. 2001, ApJ, 560, 970
 Djorgovsky, S., & Meylan, G. 1993, in: Structure and Dynamics of Globular Clusters, ASP Conf.Ser. 50, eds. G. Meylan and S. Djorgovski (San Francisco: A.S.P.), 325
 Harris, W. E. 1996, AJ 112, 1487
 Harris, W. E., & van den Bergh, S. 1984, AJ, 89, 1816
 Holland, S., & Harris W. E. 1992, AJ, 103, 131
 Kim, Y., Demarque, P., Yi, S. K., & Alexander, D. R. 2002, ApJS, 143, 499
 King, I. 1962, AJ, 67, 471
 Mackey, A. D., & Gilmore, G. F. 2004, MNRAS, 355, 504
 Mackey, A. D., & van den Bergh, S. 2005, MNRAS, 360, 631
 Madore, B. F., & Freedman, W. L. 1989, ApJ, 340, 812
 Mashchenko, S., & Sills, A. 2005, ApJ, 619, 243
 Milgrom, M. 1983, ApJ, 270, 365
 Ortolani, S., & Gratton, R. G. 1989, A&AS, 79, 155
 Sarajedini, A. 1997, AJ, 113, 682
 Schlegel, D. J., Finkbeiner, D. P., & Davis, M. 1998, ApJ, 500, 525
 Searle, L., & Zinn, R. 1978, ApJ, 225, 357
 Sohn, Y.-J., Park, J.-H., Rey, S.-C., et al. 2003, AJ, 126, 803
 Stetson, P. B. 1987, PASP, 99, 191
 Stetson, P. B. 1992, in: Astronomical Data Analysis Software and Systems I, ASP Conf.Ser. 25, eds. D.M. Worrall, C. Biemesderfer, and J. Barnes, (San Francisco: A.S.P.), 297
 Stetson, P. B., Bolte, M., Harris, W. E., et al. 1999, AJ, 117, 247
 Suntzeff, N., Olszewski, E., & Stetson, P. B. 1985, AJ, 90, 1481
 Trager, S. C., Djorgovski, S., & King I. R. 1993, in Structure and Dynamics of Globular Clusters, ASP Conf.Ser. 50, eds. S.G. Djorgovski and G. Meylan (San Francisco: A.S.P.), 347
 VandenBerg, D.A. 2000, ApJS, 129, 315
 van den Bergh, S., & Mackey, A. D. 2004, MNRAS, 354, 713
 van den Bergh, S., Morbey, C., & Pazder J. 1991, ApJ, 375, 594
 Webbink, R. F. 1985, in: Dynamics of Star Clusters, IAU Symposium 113, eds. J. Goodman and P. Hut, (Dordrecht: Reidel), 541
 Zinn, R. 1985, ApJ, 293, 424
 Zinn, R. 1993, in: The Globular Cluster-Galaxy Connection, ASP Conf.Ser. 48, eds. G.H. Smith and J.P. Brodie, (San Francisco: A.S.P.), 38

Table A.1. List of probable member stars of AM 1, ordered with increasing V magnitude.

Id	$\alpha(2000)$ [h:m:s]	$\delta(2000)$ [°:′:″]	V [mag]	$B - V$ [mag]	σ_V [mag]	σ_B [mag]	radius [′]	Type
1	03:55:02.93	-49:36:44.6	18.27	1.45	0.01	0.01	0.21	RGB
2	03:55:06.36	-49:36:09.5	19.44	1.07	0.01	0.01	1.01	RGB
3	03:55:00.64	-49:37:17.9	19.48	1.06	0.01	0.01	0.46	RGB
4	03:55:02.04	-49:36:51.7	19.51	1.02	0.01	0.01	0.07	RGB
5	03:55:06.33	-49:36:20.2	19.97	0.95	0.01	0.01	0.88	RGB
6	03:55:01.82	-49:36:39.9	20.12	0.92	0.01	0.01	0.27	RGB
7	03:55:02.15	-49:36:50.1	20.37	0.90	0.01	0.02	0.09	RGB
8	03:55:01.79	-49:41:06.0	20.43	0.73	0.01	0.01	4.18	AGB
9	03:55:04.19	-49:36:55.7	20.45	0.67	0.01	0.01	0.31	AGB
10	03:55:06.78	-49:37:02.1	20.52	0.75	0.01	0.02	0.74	AGB
11	03:55:01.31	-49:36:41.6	20.62	0.81	0.01	0.02	0.28	RGB
12	03:55:05.70	-49:37:25.9	20.63	0.67	0.01	0.01	0.75	AGB
13	03:55:03.25	-49:37:04.3	20.66	0.62	0.01	0.01	0.21	HB
14	03:55:02.36	-49:36:56.9	20.73	0.63	0.02	0.02	0.03	HB
15	03:54:59.64	-49:38:34.8	20.78	0.63	0.01	0.01	1.71	HB
16	03:54:58.65	-49:37:39.3	20.78	0.80	0.02	0.02	0.94	RGB
17	03:55:02.50	-49:37:00.7	20.80	0.65	0.03	0.04	0.09	HB
18	03:54:59.63	-49:36:45.8	20.82	0.80	0.01	0.02	0.46	RGB
19	03:55:01.04	-49:36:47.6	20.87	0.73	0.01	0.02	0.24	RGB
20	03:54:59.02	-49:36:44.9	20.87	0.79	0.01	0.02	0.56	RGB
21	03:55:01.27	-49:36:45.5	20.88	0.59	0.01	0.01	0.23	HB
22	03:55:00.68	-49:36:45.0	20.88	0.80	0.01	0.02	0.31	RGB
23	03:55:04.07	-49:37:17.0	20.88	0.64	0.02	0.02	0.46	HB
24	03:55:02.75	-49:38:43.6	20.89	0.59	0.01	0.01	1.80	HB
25	03:55:01.93	-49:36:54.6	20.89	0.52	0.02	0.02	0.06	HB
26	03:54:59.91	-49:38:01.7	20.89	0.82	0.01	0.02	1.17	RGB
27	03:55:04.57	-49:37:02.1	20.92	0.57	0.01	0.02	0.39	HB
28	03:55:02.92	-49:37:00.0	20.92	0.80	0.02	0.02	0.13	RGB
29	03:54:59.82	-49:36:56.1	20.92	0.54	0.01	0.02	0.40	HB
30	03:55:03.96	-49:36:51.9	20.93	0.54	0.01	0.02	0.28	HB
31	03:55:03.63	-49:36:45.1	20.94	0.56	0.02	0.02	0.28	HB
32	03:55:02.85	-49:36:49.7	20.94	0.64	0.02	0.02	0.13	HB
33	03:55:02.65	-49:36:44.0	20.94	0.53	0.02	0.02	0.20	HB
34	03:54:57.27	-49:36:08.0	20.96	0.57	0.01	0.01	1.13	HB
35	03:54:59.62	-49:36:40.7	20.96	0.54	0.01	0.01	0.50	HB
36	03:55:01.82	-49:37:14.8	20.98	0.55	0.02	0.02	0.33	HB
37	03:54:43.93	-49:34:34.2	20.98	0.75	0.02	0.02	3.80	RGB
38	03:55:02.13	-49:37:26.1	20.98	0.60	0.01	0.02	0.51	HB
39	03:55:01.19	-49:36:30.6	20.98	0.58	0.01	0.02	0.45	HB
40	03:54:58.67	-49:36:20.8	20.98	0.52	0.01	0.01	0.82	HB
41	03:55:03.07	-49:36:46.5	20.99	0.59	0.02	0.02	0.19	HB
42	03:55:03.54	-49:36:43.9	20.99	0.53	0.02	0.02	0.28	HB
43	03:55:01.39	-49:36:47.4	20.99	0.57	0.01	0.02	0.20	HB
44	03:54:50.84	-49:38:21.4	21.00	0.64	0.01	0.02	2.34	HB
45	03:55:04.06	-49:37:01.5	21.00	0.52	0.02	0.02	0.30	HB
46	03:55:04.85	-49:36:48.4	21.00	0.54	0.01	0.02	0.43	HB
47	03:55:06.02	-49:37:05.8	21.01	0.55	0.01	0.01	0.63	HB
48	03:55:00.81	-49:37:01.1	21.01	0.55	0.01	0.02	0.26	HB
49	03:55:01.38	-49:37:00.4	21.02	0.52	0.02	0.02	0.17	HB
50	03:55:02.01	-49:36:55.6	21.02	0.53	0.02	0.02	0.05	HB
51	03:55:04.22	-49:37:04.0	21.02	0.79	0.02	0.02	0.34	RGB
52	03:55:00.59	-49:36:50.9	21.02	0.55	0.02	0.02	0.29	HB
53	03:54:59.20	-49:36:10.3	21.02	0.53	0.02	0.01	0.90	HB
54	03:55:01.43	-49:36:35.8	21.02	0.52	0.02	0.02	0.36	HB
55	03:55:02.35	-49:36:55.9	21.03	0.72	0.03	0.03	0.01	RGB
56	03:55:02.30	-49:36:37.9	21.04	0.56	0.01	0.02	0.29	HB
57	03:55:01.43	-49:37:05.7	21.04	0.77	0.01	0.02	0.22	RGB
58	03:55:07.14	-49:36:39.7	21.04	0.76	0.01	0.02	0.83	RGB
59	03:54:59.93	-49:36:51.5	21.06	0.49	0.02	0.02	0.39	HB
60	03:55:03.35	-49:37:12.9	21.09	0.53	0.02	0.02	0.34	HB
61	03:55:01.28	-49:37:06.2	21.17	0.75	0.02	0.03	0.24	RGB
62	03:54:58.25	-49:38:14.7	21.17	0.71	0.01	0.02	1.47	RGB
63	03:55:02.59	-49:37:02.2	21.17	0.77	0.02	0.04	0.12	RGB
64	03:55:03.77	-49:38:03.4	21.30	0.41	0.02	0.02	1.16	HB
65	03:55:02.97	-49:37:13.1	21.31	0.68	0.03	0.02	0.31	RGB
66	03:55:01.21	-49:36:20.9	21.33	0.73	0.01	0.02	0.60	RGB
67	03:55:02.67	-49:36:46.7	21.37	0.69	0.02	0.03	0.16	RGB
68	03:55:04.21	-49:37:29.2	21.40	0.73	0.02	0.03	0.64	RGB
69	03:55:03.66	-49:36:48.4	21.41	0.79	0.02	0.03	0.25	RGB
70	03:55:12.00	-49:34:51.1	21.46	0.68	0.03	0.03	2.60	RGB
71	03:55:01.91	-49:36:27.5	21.47	0.73	0.02	0.03	0.47	RGB
72	03:55:09.89	-49:37:36.2	21.50	0.43	0.02	0.02	1.40	HB
73	03:55:01.58	-49:36:56.1	21.58	0.73	0.03	0.03	0.12	RGB
74	03:55:03.45	-49:36:04.8	21.67	0.76	0.02	0.02	0.87	RGB
75	03:55:02.47	-49:37:05.0	21.69	0.67	0.03	0.04	0.16	RGB
76	03:55:03.23	-49:36:51.6	21.73	0.70	0.04	0.04	0.16	RGB
77	03:55:06.81	-49:37:38.8	21.85	0.66	0.03	0.03	1.03	RGB
78	03:55:02.10	-49:37:21.2	21.85	0.75	0.03	0.04	0.43	RGB
79	03:55:03.47	-49:36:50.0	21.87	0.70	0.08	0.07	0.21	RGB
80	03:55:01.81	-49:37:03.9	21.88	0.78	0.04	0.04	0.16	RGB
81	03:55:02.31	-49:37:02.3	21.91	0.77	0.03	0.05	0.11	RGB
82	03:54:50.34	-49:34:53.5	21.95	0.72	0.03	0.04	2.81	RGB
83	03:55:03.82	-49:36:32.7	22.04	0.64	0.03	0.04	0.45	RGB
84	03:55:02.54	-49:37:19.0	22.06	0.68	0.03	0.04	0.39	RGB
85	03:55:04.96	-49:37:12.8	22.08	0.66	0.03	0.05	0.52	RGB
86	03:55:02.63	-49:37:18.5	22.14	0.71	0.04	0.04	0.39	RGB
87	03:55:04.29	-49:36:38.6	22.17	0.65	0.03	0.04	0.43	RGB
88	03:55:00.41	-49:37:00.4	22.22	0.66	0.03	0.04	0.32	RGB
89	03:55:03.87	-49:35:48.2	22.33	0.62	0.03	0.04	1.15	RGB
90	03:54:59.31	-49:36:15.6	22.34	0.65	0.04	0.05	0.82	RGB

Table A.1. (continued)

Id	$\alpha(2000)$ [h:m:s]	$\delta(2000)$ [$^{\circ}$: $'$: $''$]	V [mag]	$B - V$ [mag]	σ_V [mag]	σ_B [mag]	radius [$'$]	Type
91	03:55:02.00	-49:37:09.0	22.35	0.68	0.04	0.06	0.23	RGB
92	03:55:04.18	-49:37:46.5	22.36	0.64	0.04	0.05	0.90	RGB
93	03:54:51.97	-49:35:54.4	22.39	0.64	0.06	0.05	1.96	RGB
94	03:54:58.27	-49:36:28.0	22.45	0.62	0.04	0.04	0.80	RGB
95	03:55:05.75	-49:36:03.1	22.47	0.69	0.03	0.06	1.04	RGB
96	03:55:02.60	-49:37:11.6	22.53	0.68	0.04	0.06	0.27	RGB
97	03:55:10.81	-49:40:31.9	22.56	0.71	0.06	0.06	3.86	RGB
98	03:55:02.88	-49:36:31.9	22.58	0.65	0.04	0.05	0.40	RGB
99	03:55:03.88	-49:36:58.2	22.60	0.63	0.06	0.07	0.26	RGB
100	03:54:59.98	-49:36:53.9	22.61	0.68	0.05	0.06	0.38	RGB
101	03:54:43.96	-49:37:59.2	22.61	0.73	0.05	0.07	3.15	RGB
102	03:54:59.13	-49:37:12.9	22.67	0.63	0.06	0.07	0.59	RGB
103	03:55:01.82	-49:37:09.1	22.69	0.62	0.04	0.07	0.24	RGB
104	03:55:22.06	-49:36:08.5	22.69	0.63	0.05	0.07	3.30	RGB
105	03:55:02.10	-49:36:45.8	22.75	0.66	0.06	0.07	0.16	RGB
106	03:54:49.76	-49:37:22.8	22.77	0.59	0.07	0.06	2.08	RGB
107	03:55:05.37	-49:36:44.6	22.77	0.62	0.05	0.09	0.53	RGB
108	03:55:02.05	-49:37:01.3	22.78	0.60	0.05	0.10	0.10	RGB
109	03:55:04.44	-49:36:37.5	22.89	0.70	0.05	0.10	0.46	RGB
110	03:55:01.53	-49:37:20.8	22.91	0.67	0.06	0.08	0.44	RGB

Table A.2. List of probable member stars of Pal 3, ordered with increasing V magnitude.

Id	$\alpha(2000)$ [h:m:s]	$\delta(2000)$ [$^{\circ}$: $'$: $''$]	V [mag]	$B - V$ [mag]	σ_V [mag]	σ_B [mag]	radius [$'$]	Type
1	10:05:36.24	00:03:59.9	18.05	1.16	0.01	0.01	1.11	RGB
2	10:05:31.57	00:04:17.0	18.25	1.13	0.02	0.01	0.10	RGB
3	10:05:37.08	00:04:27.9	18.37	1.12	0.01	0.01	1.29	RGB
4	10:05:29.71	00:05:39.2	18.64	0.95	0.02	0.01	1.46	AGB?
5	10:05:31.05	00:04:17.3	18.76	1.00	0.01	0.01	0.23	RGB
6	10:05:34.63	00:04:06.9	19.30	0.89	0.01	0.01	0.69	RGB
7	10:05:21.69	00:07:35.2	19.30	0.81	0.02	0.01	4.17	AGB?
8	10:05:31.84	00:04:16.5	19.34	0.86	0.02	0.01	0.04	RGB
9	10:05:32.87	00:04:36.1	19.37	0.88	0.02	0.01	0.38	RGB
10	10:05:33.19	00:03:57.1	19.42	0.88	0.02	0.01	0.47	RGB
11	10:05:27.72	00:05:08.8	19.54	0.85	0.02	0.01	1.35	RGB
12	10:05:31.12	00:04:16.9	19.59	0.89	0.02	0.01	0.21	RGB
13	10:05:32.91	00:04:26.1	19.80	0.85	0.02	0.01	0.27	RGB
14	10:05:32.59	00:04:32.3	19.85	0.82	0.02	0.01	0.29	RGB
15	10:05:32.73	00:04:36.7	19.97	0.81	0.02	0.01	0.37	RGB
16	10:05:29.92	00:04:53.9	20.04	0.77	0.04	0.03	0.78	RGB
17	10:05:28.29	00:04:37.7	20.08	0.61	0.01	0.01	0.97	RGB
18	10:05:23.96	00:04:24.5	20.12	0.71	0.01	0.01	2.00	AGB
19	10:05:30.25	00:03:37.6	20.14	0.80	0.01	0.01	0.80	RGB
20	10:05:30.36	00:05:29.6	20.18	0.59	0.02	0.01	1.26	AGB
21	10:05:28.83	00:04:36.5	20.22	0.79	0.01	0.01	0.84	RGB
22	10:05:28.79	00:03:45.5	20.22	0.78	0.01	0.01	0.96	RGB
23	10:05:29.97	00:04:03.8	20.26	0.78	0.01	0.01	0.55	RGB
24	10:05:30.44	00:03:38.1	20.27	0.28	0.01	0.01	0.77	HB
25	10:05:34.35	00:04:39.2	20.27	0.65	0.01	0.01	0.70	AGB
26	10:05:33.82	00:04:18.2	20.28	0.34	0.02	0.01	0.47	HB
27	10:05:21.94	00:04:06.3	20.30	0.33	0.02	0.01	2.51	HB
28	10:05:30.07	00:02:04.7	20.31	0.80	0.02	0.01	2.27	RGB
29	10:05:31.49	00:04:27.7	20.31	0.76	0.02	0.01	0.20	RGB
30	10:05:31.35	00:04:14.4	20.33	0.28	0.02	0.01	0.16	HB
31	10:05:35.79	00:03:34.3	20.33	0.50	0.01	0.01	1.20	HB
32	10:05:32.63	00:04:21.3	20.39	0.37	0.02	0.01	0.18	HB
33	10:05:35.91	00:05:10.3	20.39	0.39	0.01	0.01	1.32	HB
34	10:05:33.32	00:04:38.0	20.40	0.45	0.02	0.01	0.48	HB
35	10:05:27.59	00:05:00.0	20.42	0.41	0.02	0.01	1.30	HB
36	10:05:39.49	00:00:10.8	20.43	0.64	0.03	0.02	4.53	AGB
37	10:05:34.47	00:03:57.1	20.43	0.45	0.01	0.01	0.72	HB
38	10:05:27.77	00:04:35.5	20.43	0.43	0.01	0.01	1.09	HB
39	10:05:30.44	00:04:22.9	20.44	0.46	0.02	0.01	0.39	HB
40	10:05:28.24	00:03:34.3	20.45	0.29	0.01	0.01	1.18	HB
41	10:05:29.61	00:04:21.3	20.45	0.51	0.01	0.01	0.59	HB
42	10:05:34.00	00:04:27.4	20.45	0.49	0.01	0.01	0.54	HB
43	10:05:35.85	00:04:15.8	20.46	0.44	0.01	0.01	0.98	HB
44	10:05:29.65	00:04:12.0	20.47	0.35	0.04	0.01	0.58	HB
45	10:05:27.39	00:05:09.7	20.47	0.38	0.02	0.01	1.43	HB
46	10:05:31.53	00:04:40.5	20.47	0.45	0.01	0.01	0.39	HB
47	10:05:28.80	00:04:10.9	20.48	0.51	0.01	0.01	0.80	HB
48	10:05:29.12	00:03:45.8	20.49	0.49	0.02	0.01	0.89	HB
49	10:05:35.95	00:05:05.6	20.50	0.48	0.01	0.01	1.28	HB
50	10:05:31.82	00:04:25.4	20.51	0.75	0.02	0.01	0.13	RGB
51	10:05:28.34	00:04:48.7	20.54	0.76	0.01	0.01	1.04	RGB
52	10:05:36.69	00:03:15.7	20.54	0.39	0.01	0.01	1.58	HB
53	10:05:31.54	00:04:21.7	20.54	0.41	0.02	0.01	0.12	HB
54	10:05:38.09	00:04:53.3	20.61	0.74	0.01	0.01	1.64	RGB
55	10:05:30.53	00:04:37.3	20.61	0.47	0.02	0.01	0.48	HB
56	10:05:33.21	00:05:06.2	20.63	0.75	0.02	0.01	0.86	RGB
57	10:05:35.28	00:03:43.1	20.70	0.40	0.01	0.01	1.02	HB
58	10:05:21.84	00:01:05.8	20.70	0.49	0.04	0.03	4.08	HB
59	10:05:33.41	00:04:28.5	20.70	0.42	0.02	0.01	0.40	HB
60	10:05:32.37	00:04:12.1	20.72	0.72	0.02	0.01	0.14	RGB
61	10:05:20.31	00:07:37.3	20.76	0.42	0.02	0.01	4.42	HB

Table A.2. (continued)

Id	$\alpha(2000)$ [h:m:s]	$\delta(2000)$ [$^{\circ}$: $'$: $''$]	V [mag]	$B - V$ [mag]	σ_V [mag]	σ_B [mag]	radius [$'$]	Type
62	10:05:30.12	00:04:46.0	20.86	0.72	0.02	0.01	0.65	RGB
63	10:05:30.87	00:04:39.9	20.92	0.69	0.02	0.02	0.45	RGB
64	10:05:31.51	00:04:54.5	20.95	0.68	0.02	0.01	0.62	RGB
65	10:05:31.88	00:06:17.2	20.96	0.66	0.02	0.02	1.99	RGB
66	10:05:25.51	00:04:15.7	21.01	0.71	0.02	0.01	1.61	RGB
67	10:05:35.85	00:04:54.5	21.02	0.70	0.01	0.01	1.15	RGB
68	10:05:32.48	00:04:13.6	21.03	0.72	0.02	0.02	0.15	RGB
69	10:05:42.34	00:01:04.2	21.05	0.69	0.04	0.03	4.14	RGB
70	10:05:33.10	00:04:11.9	21.07	0.70	0.02	0.02	0.31	RGB
71	10:05:29.63	00:04:23.8	21.10	0.71	0.02	0.02	0.59	RGB
72	10:05:33.12	00:04:36.1	21.14	0.73	0.03	0.02	0.42	RGB
73	10:05:30.90	00:04:48.5	21.17	0.66	0.04	0.03	0.57	RGB
74	10:05:33.18	00:03:59.9	21.22	0.63	0.02	0.02	0.43	RGB
75	10:05:30.90	00:04:33.9	21.28	0.63	0.02	0.02	0.37	RGB
76	10:05:31.21	00:05:03.3	21.32	0.70	0.02	0.02	0.78	RGB
77	10:05:32.30	00:03:55.3	21.36	0.73	0.02	0.03	0.39	RGB
78	10:05:37.93	00:04:07.8	21.42	0.72	0.02	0.01	1.50	RGB
79	10:05:32.77	00:04:15.2	21.43	0.66	0.02	0.02	0.21	RGB
80	10:05:29.94	00:04:28.5	21.48	0.68	0.02	0.01	0.53	RGB
81	10:05:33.44	00:04:25.2	21.51	0.70	0.02	0.02	0.39	RGB
82	10:05:25.75	00:04:20.8	21.52	0.66	0.02	0.01	1.55	RGB
83	10:05:30.78	00:04:29.1	21.57	0.61	0.03	0.02	0.35	RGB
84	10:05:30.89	00:03:51.0	21.58	0.65	0.03	0.02	0.52	RGB
85	10:05:38.12	00:05:00.2	21.63	0.67	0.02	0.01	1.70	RGB
86	10:05:29.29	00:04:24.8	21.66	0.69	0.02	0.02	0.68	RGB
87	10:05:29.48	00:03:20.0	21.70	0.68	0.02	0.02	1.15	RGB
88	10:05:32.08	00:04:16.7	21.71	0.65	0.03	0.02	0.04	RGB
89	10:05:32.02	00:04:51.4	21.73	0.66	0.02	0.02	0.56	RGB
90	10:05:28.88	00:04:12.1	21.76	0.66	0.03	0.02	0.77	RGB
91	10:05:28.96	00:04:20.4	21.77	0.69	0.02	0.01	0.75	RGB
92	10:05:31.12	00:04:32.2	21.78	0.62	0.03	0.03	0.31	RGB
93	10:05:32.00	00:04:22.0	21.80	0.69	0.03	0.03	0.07	RGB
94	10:05:30.37	00:04:03.1	21.81	0.65	0.05	0.04	0.47	RGB
95	10:05:33.34	00:04:18.2	21.83	0.65	0.04	0.02	0.35	RGB
96	10:05:31.61	00:04:12.2	21.88	0.62	0.04	0.03	0.13	RGB
97	10:05:32.43	00:03:59.8	21.89	0.59	0.03	0.02	0.33	RGB
98	10:05:29.36	00:08:33.4	21.92	0.66	0.04	0.03	4.31	RGB
99	10:05:31.72	00:04:19.8	21.92	0.67	0.03	0.02	0.07	RGB
100	10:05:35.42	00:03:07.8	21.92	0.62	0.02	0.02	1.46	RGB
101	10:05:33.85	00:06:17.2	21.93	0.64	0.03	0.03	2.04	RGB
102	10:05:33.59	00:02:53.0	21.93	0.65	0.02	0.01	1.48	RGB
103	10:05:30.03	00:04:28.1	21.94	0.70	0.02	0.02	0.51	RGB
104	10:05:32.34	00:04:21.4	21.98	0.63	0.03	0.03	0.11	RGB
105	10:05:33.53	00:04:20.9	21.99	0.68	0.03	0.02	0.40	RGB
106	10:05:29.06	00:04:29.4	22.02	0.60	0.03	0.02	0.75	RGB
107	10:05:37.11	00:04:58.6	22.02	0.65	0.02	0.02	1.46	RGB
108	10:05:36.87	00:03:42.5	22.04	0.64	0.03	0.03	1.36	RGB
109	10:05:33.07	00:04:09.4	22.04	0.69	0.03	0.02	0.32	RGB
110	10:05:23.81	00:04:22.7	22.07	0.64	0.02	0.02	2.04	RGB
111	10:05:40.33	00:09:14.9	22.09	0.60	0.04	0.03	5.37	RGB
112	10:05:27.96	00:04:26.0	22.10	0.71	0.03	0.02	1.01	RGB
113	10:05:21.85	00:07:41.0	22.10	0.58	0.04	0.03	4.22	RGB
114	10:05:41.53	00:05:45.4	22.14	0.67	0.05	0.03	2.80	RGB
115	10:05:33.00	00:06:34.6	22.16	0.59	0.04	0.03	2.29	RGB
116	10:05:31.59	00:03:28.9	22.17	0.59	0.03	0.02	0.82	RGB
117	10:05:29.98	00:04:27.1	22.18	0.64	0.04	0.04	0.52	RGB
118	10:05:28.18	00:04:35.3	22.18	0.57	0.03	0.02	0.98	RGB
119	10:05:28.65	00:05:48.8	22.18	0.65	0.03	0.02	1.72	RGB
120	10:05:34.50	00:04:42.8	22.20	0.70	0.03	0.02	0.76	RGB
121	10:05:30.95	00:04:12.4	22.21	0.59	0.04	0.03	0.27	RGB
122	10:05:33.34	00:05:35.4	22.23	0.70	0.04	0.04	1.34	RGB
123	10:05:32.15	00:04:51.1	22.23	0.63	0.04	0.02	0.55	RGB
124	10:05:30.30	00:04:07.6	22.23	0.63	0.04	0.03	0.45	RGB
125	10:05:33.96	00:03:30.5	22.24	0.63	0.04	0.03	0.94	RGB
126	10:05:27.88	00:08:29.6	22.26	0.60	0.05	0.04	4.31	RGB
127	10:05:31.40	00:03:25.4	22.26	0.64	0.05	0.03	0.89	RGB
128	10:05:31.84	00:04:42.6	22.27	0.70	0.04	0.03	0.41	RGB
129	10:05:30.64	00:03:16.8	22.30	0.63	0.04	0.03	1.07	RGB
130	10:05:31.42	00:03:36.1	22.30	0.65	0.04	0.03	0.71	RGB
131	10:05:32.78	00:04:09.7	22.30	0.64	0.06	0.04	0.25	RGB
132	10:05:29.59	00:04:26.3	22.34	0.64	0.03	0.03	0.61	RGB
133	10:05:31.92	00:05:08.9	22.35	0.69	0.05	0.04	0.85	RGB
134	10:05:34.04	00:03:44.3	22.35	0.56	0.04	0.04	0.77	RGB
135	10:05:28.01	00:04:06.1	22.36	0.66	0.04	0.03	1.00	RGB
136	10:05:32.55	00:03:34.7	22.39	0.67	0.04	0.03	0.74	RGB
137	10:05:32.12	00:04:57.7	22.40	0.71	0.06	0.05	0.66	RGB
138	10:05:29.26	00:03:44.5	22.41	0.62	0.04	0.03	0.88	RGB
139	10:05:30.79	00:04:24.1	22.44	0.62	0.05	0.03	0.31	RGB
140	10:05:36.89	00:06:35.1	22.44	0.56	0.05	0.03	2.60	RGB
141	10:05:37.92	00:02:41.4	22.45	0.57	0.07	0.07	2.20	RGB
142	10:05:30.71	00:03:46.7	22.48	0.66	0.04	0.04	0.61	RGB
143	10:05:32.34	00:04:05.6	22.48	0.62	0.04	0.04	0.23	RGB
144	10:05:33.16	00:04:33.6	22.48	0.71	0.05	0.04	0.40	RGB
145	10:05:33.91	00:04:48.9	22.48	0.59	0.03	0.02	0.71	RGB
146	10:05:30.26	00:03:45.6	22.52	0.69	0.05	0.04	0.69	RGB
147	10:05:37.41	00:06:11.1	22.52	0.56	0.05	0.03	2.33	RGB
148	10:05:28.19	00:03:26.2	22.52	0.66	0.04	0.04	1.28	RGB
149	10:05:24.98	00:04:14.3	22.52	0.69	0.04	0.04	1.74	RGB
150	10:05:32.97	00:04:37.8	22.53	0.55	0.05	0.03	0.42	RGB
151	10:05:32.30	00:03:22.6	22.60	0.67	0.05	0.03	0.93	RGB
152	10:05:27.74	00:03:19.7	22.62	0.59	0.04	0.04	1.43	RGB
153	10:05:29.79	00:03:46.0	22.62	0.67	0.05	0.04	0.76	RGB

Table A.3. List of probable member stars of Pal 14, ordered with increasing V magnitude.

Id	$\alpha(2000)$ [h:m:s]	$\delta(2000)$ [°:′:″]	V [mag]	$B - V$ [mag]	σ_V [mag]	σ_B [mag]	radius [′]	Type
1	16:11:05.81	14:57:45.1	17.37	1.39	0.02	0.01	1.28	RGB
2	16:10:58.73	14:56:48.7	17.77	1.29	0.02	0.01	0.80	RGB
3	16:10:54.90	14:58:36.7	18.23	1.07	0.01	0.01	1.80	AGB?
4	16:11:04.98	14:53:32.3	18.48	1.10	0.02	0.01	4.07	RGB
5	16:10:59.24	14:57:22.5	18.52	0.99	0.01	0.01	0.35	AGB?
6	16:10:53.36	14:56:45.4	18.56	1.04	0.01	0.01	1.90	RGB
7	16:10:54.04	14:57:05.6	18.70	1.03	0.01	0.01	1.64	RGB
8	16:10:56.90	14:57:56.5	18.84	0.99	0.01	0.01	1.02	RGB
9	16:11:01.40	14:57:60.0	19.05	0.99	0.01	0.01	0.56	RGB
10	16:11:05.89	14:58:43.2	19.19	0.93	0.02	0.01	1.78	RGB
11	16:11:06.00	14:55:39.1	19.37	0.95	0.01	0.01	2.23	RGB
12	16:10:56.21	14:56:32.7	19.41	0.90	0.01	0.01	1.42	RGB
13	16:10:56.98	14:56:25.8	19.44	0.92	0.01	0.01	1.37	RGB
14	16:10:59.24	14:57:19.7	19.50	0.90	0.02	0.01	0.37	RGB
15	16:10:55.84	14:57:43.4	19.60	0.69	0.01	0.01	1.19	AGB
16	16:10:59.62	15:01:32.9	19.68	0.81	0.02	0.01	4.09	RGB
17	16:11:00.58	14:56:59.1	19.76	0.86	0.01	0.01	0.48	RGB
18	16:11:03.91	14:56:34.3	19.77	0.59	0.01	0.01	1.19	AGB
19	16:11:01.01	14:55:23.1	19.78	0.69	0.01	0.01	2.09	AGB
20	16:11:07.42	14:57:43.2	19.86	0.86	0.01	0.01	1.65	RGB
21	16:10:52.81	14:55:38.9	19.87	0.84	0.01	0.01	2.62	RGB
22	16:10:56.17	14:55:48.1	19.88	0.46	0.01	0.01	1.99	HB
23	16:11:02.52	14:56:49.7	19.88	0.62	0.01	0.01	0.78	HB
24	16:11:10.09	14:55:54.9	19.89	0.88	0.02	0.01	2.76	RGB
25	16:11:04.45	14:56:14.4	19.90	0.65	0.01	0.01	1.53	HB
26	16:10:59.32	14:57:25.9	19.92	0.84	0.02	0.01	0.32	RGB
27	16:11:16.22	15:00:07.1	19.92	0.47	0.02	0.01	4.60	HB
28	16:10:59.89	14:53:27.8	19.92	0.92	0.03	0.02	4.01	RGB
29	16:11:12.60	14:56:55.2	19.93	0.46	0.02	0.01	2.94	HB
30	16:11:13.56	14:57:58.2	19.95	0.85	0.02	0.01	3.16	RGB
31	16:11:01.64	14:59:47.8	19.95	0.80	0.02	0.02	2.34	RGB
32	16:10:56.39	14:57:25.1	19.96	0.84	0.01	0.02	1.03	RGB
33	16:11:09.37	14:57:37.5	19.97	0.61	0.02	0.01	2.11	HB
34	16:10:58.62	14:57:40.3	19.97	0.83	0.01	0.01	0.53	RGB
35	16:11:09.57	15:01:07.7	19.98	0.58	0.02	0.02	4.25	HB
36	16:10:59.15	14:57:38.0	19.98	0.76	0.01	0.01	0.40	HB?
37	16:10:56.20	14:57:34.4	19.99	0.61	0.01	0.01	1.08	HB
38	16:11:01.76	14:58:06.8	19.99	0.61	0.01	0.01	0.70	HB
39	16:10:59.72	14:57:45.6	20.00	0.58	0.01	0.01	0.37	HB
40	16:10:59.15	14:55:01.8	20.03	0.67	0.02	0.02	2.46	HB
41	16:11:00.81	14:57:53.4	20.03	0.58	0.02	0.01	0.42	HB
42	16:10:53.24	14:57:50.2	20.03	0.55	0.01	0.01	1.83	HB
43	16:10:53.08	14:56:22.9	20.03	0.55	0.02	0.01	2.13	HB
44	16:10:55.09	14:57:44.3	20.04	0.60	0.01	0.01	1.37	HB
45	16:11:01.49	14:57:46.0	20.04	0.58	0.02	0.01	0.36	HB
46	16:11:08.53	14:53:09.0	20.04	0.50	0.02	0.01	4.72	HB
47	16:10:53.97	14:56:35.4	20.06	0.55	0.01	0.02	1.84	HB
48	16:11:03.24	14:57:44.9	20.06	0.62	0.01	0.01	0.69	HB
49	16:11:16.01	14:54:36.2	20.07	0.64	0.03	0.02	4.69	HB
50	16:11:02.83	14:57:09.0	20.07	0.56	0.01	0.01	0.62	HB
51	16:10:59.37	14:57:43.5	20.07	0.57	0.01	0.01	0.40	HB
52	16:10:53.27	14:56:27.2	20.07	0.54	0.01	0.01	2.05	HB
53	16:11:00.38	14:57:40.7	20.08	0.55	0.02	0.01	0.22	HB
54	16:11:09.51	14:59:43.9	20.08	0.57	0.02	0.01	3.12	HB
55	16:10:59.25	14:57:14.0	20.08	0.58	0.01	0.01	0.41	HB
56	16:10:59.65	14:56:43.4	20.11	0.59	0.01	0.02	0.78	HB
57	16:11:00.94	14:58:50.3	20.11	0.41	0.01	0.01	1.37	HB
58	16:11:01.91	14:57:53.2	20.11	0.84	0.01	0.02	0.52	RGB
59	16:10:56.97	14:57:28.0	20.11	0.56	0.01	0.01	0.89	HB
60	16:10:57.39	14:56:01.3	20.13	0.86	0.02	0.02	1.65	RGB
61	16:11:01.71	14:57:36.9	20.14	0.57	0.01	0.01	0.30	HB
62	16:10:59.47	14:56:03.6	20.19	0.67	0.01	0.01	1.44	HB
63	16:11:13.75	14:54:18.3	20.24	0.88	0.04	0.02	4.48	RGB
64	16:10:59.47	14:58:02.1	20.28	0.84	0.02	0.02	0.63	RGB
65	16:10:59.65	14:55:42.4	20.30	0.79	0.01	0.02	1.78	RGB
66	16:10:58.97	14:55:28.4	20.33	0.82	0.02	0.01	2.04	RGB
67	16:10:54.49	14:57:19.5	20.34	0.82	0.01	0.01	1.49	RGB
68	16:10:59.66	14:58:18.5	20.38	0.83	0.02	0.02	0.87	RGB
69	16:11:01.04	14:58:32.6	20.39	0.83	0.02	0.02	1.08	RGB
70	16:11:15.80	14:57:55.6	20.41	0.91	0.02	0.02	3.69	RGB
71	16:10:57.31	14:59:21.7	20.42	0.44	0.02	0.01	2.06	HB?
72	16:11:08.15	14:57:40.5	20.48	0.77	0.02	0.02	1.82	RGB
73	16:11:07.45	14:58:30.7	20.51	0.79	0.02	0.02	1.95	RGB
74	16:11:03.28	14:58:04.1	20.54	0.81	0.02	0.02	0.87	RGB
75	16:10:56.94	14:57:10.5	20.58	0.78	0.02	0.02	0.94	RGB
76	16:10:57.67	14:57:19.1	20.60	0.74	0.01	0.02	0.73	RGB
77	16:10:59.59	14:57:20.1	20.67	0.74	0.01	0.02	0.29	RGB
78	16:11:11.43	14:58:09.6	20.67	0.81	0.02	0.02	2.69	RGB
79	16:11:00.93	14:57:31.7	20.83	0.74	0.02	0.03	0.09	RGB
80	16:10:58.97	14:53:23.0	20.85	0.81	0.03	0.02	4.11	RGB
81	16:11:07.10	14:58:17.8	20.85	0.78	0.02	0.02	1.76	RGB
82	16:11:01.63	14:55:27.6	20.90	0.77	0.02	0.03	2.02	RGB
83	16:11:00.90	14:58:06.8	20.97	0.70	0.02	0.03	0.65	RGB
84	16:10:59.36	14:56:58.3	20.98	0.76	0.02	0.03	0.59	RGB
85	16:11:17.29	14:56:19.9	21.00	0.72	0.02	0.02	4.18	RGB
86	16:10:54.40	14:58:31.1	21.02	0.74	0.02	0.02	1.84	RGB
87	16:10:54.08	14:58:33.6	21.05	0.77	0.02	0.03	1.93	RGB
88	16:11:02.26	14:58:25.2	21.10	0.82	0.02	0.04	1.03	RGB
89	16:11:06.41	14:53:22.1	21.12	0.85	0.02	0.04	4.33	RGB
90	16:11:09.75	14:57:55.8	21.18	0.75	0.02	0.04	2.25	RGB

Table A.3. (continued)

Id	$\alpha(2000)$ [h:m:s]	$\delta(2000)$ [°:′:″]	V [mag]	$B - V$ [mag]	σ_V [mag]	σ_B [mag]	radius [′]	Type
91	16:11:05.62	14:58:45.8	21.18	0.69	0.02	0.03	1.77	RGB
92	16:11:07.25	14:57:11.9	21.21	0.79	0.02	0.04	1.62	RGB
93	16:11:02.05	14:58:21.3	21.21	0.70	0.02	0.04	0.95	RGB
94	16:10:57.26	14:57:35.4	21.23	0.71	0.02	0.03	0.83	RGB
95	16:11:00.23	14:58:02.6	21.23	0.72	0.02	0.03	0.58	RGB
96	16:10:59.37	14:57:35.3	21.24	0.72	0.02	0.03	0.33	RGB
97	16:11:03.92	14:56:21.7	21.29	0.70	0.03	0.03	1.36	RGB
98	16:10:59.12	14:56:52.0	21.30	0.74	0.02	0.04	0.70	RGB
99	16:11:05.63	14:59:20.3	21.30	0.76	0.03	0.05	2.22	RGB
100	16:11:00.25	14:58:12.4	21.35	0.78	0.03	0.04	0.75	RGB
101	16:11:08.20	14:58:53.5	21.40	0.69	0.02	0.03	2.31	RGB
102	16:10:59.70	14:57:29.8	21.41	0.77	0.02	0.04	0.23	RGB
103	16:11:01.68	14:57:09.4	21.42	0.73	0.02	0.04	0.40	RGB
104	16:10:58.82	14:57:17.6	21.43	0.76	0.02	0.04	0.47	RGB
105	16:11:00.37	14:57:45.6	21.47	0.73	0.03	0.04	0.30	RGB
106	16:11:01.58	14:58:49.8	21.48	0.74	0.02	0.04	1.38	RGB
107	16:10:57.76	14:55:27.3	21.54	0.81	0.03	0.05	2.13	RGB
108	16:11:00.59	14:57:03.1	21.56	0.67	0.03	0.05	0.42	RGB
109	16:11:01.72	14:57:56.4	21.59	0.75	0.02	0.04	0.54	RGB
110	16:11:03.46	14:56:35.5	21.65	0.75	0.02	0.05	1.11	RGB
111	16:11:02.28	14:58:13.4	21.66	0.63	0.03	0.04	0.85	RGB
112	16:11:00.03	14:57:27.7	21.72	0.78	0.03	0.05	0.15	RGB
113	16:10:55.84	14:56:54.1	21.72	0.73	0.03	0.06	1.29	RGB
114	16:11:15.66	14:59:26.6	21.74	0.74	0.03	0.06	4.13	RGB
115	16:11:02.13	14:57:17.1	21.75	0.79	0.05	0.05	0.40	RGB
116	16:11:01.79	14:55:48.3	21.76	0.68	0.03	0.05	1.68	RGB
117	16:11:00.66	14:57:03.8	21.78	0.68	0.03	0.04	0.40	RGB
118	16:10:58.93	14:57:53.1	21.80	0.70	0.02	0.05	0.59	RGB
119	16:11:01.50	14:58:28.3	21.82	0.71	0.03	0.05	1.02	RGB
120	16:10:57.79	14:56:23.9	21.83	0.69	0.03	0.05	1.27	RGB
121	16:11:04.03	15:02:01.1	21.84	0.78	0.03	0.06	4.62	RGB
122	16:10:58.53	14:57:02.2	21.85	0.65	0.03	0.05	0.67	RGB
123	16:11:01.37	14:57:40.2	21.87	0.78	0.03	0.05	0.27	RGB
124	16:10:55.65	14:57:12.9	21.92	0.64	0.03	0.06	1.23	RGB
125	16:11:01.20	14:58:37.3	21.92	0.66	0.02	0.04	1.16	RGB
126	16:11:00.14	14:58:22.3	21.93	0.67	0.04	0.06	0.91	RGB
127	16:11:05.39	14:56:59.9	21.94	0.69	0.04	0.07	1.24	RGB
128	16:10:55.79	14:58:02.7	22.00	0.72	0.04	0.06	1.31	RGB
129	16:10:59.39	15:01:17.9	22.01	0.62	0.04	0.05	3.84	RGB
130	16:11:00.63	14:58:27.8	22.01	0.78	0.03	0.07	0.99	RGB
131	16:10:59.19	14:56:02.5	22.02	0.71	0.03	0.08	1.47	RGB
132	16:11:10.01	14:58:51.7	22.06	0.75	0.02	0.04	2.66	RGB
133	16:11:02.13	14:57:03.0	22.08	0.72	0.03	0.07	0.55	RGB
134	16:10:58.95	14:58:04.7	22.10	0.61	0.04	0.07	0.74	RGB
135	16:10:55.42	14:57:20.6	22.11	0.69	0.04	0.07	1.27	RGB
136	16:10:57.33	14:57:23.4	22.14	0.61	0.05	0.07	0.81	RGB
137	16:11:03.62	14:57:22.5	22.15	0.76	0.04	0.07	0.72	RGB
138	16:11:00.66	14:56:51.7	22.18	0.68	0.04	0.08	0.61	RGB
139	16:11:00.83	14:58:22.2	22.24	0.69	0.04	0.08	0.90	RGB
140	16:11:01.28	14:56:51.2	22.27	0.71	0.04	0.11	0.63	RGB
141	16:10:54.85	15:00:45.2	22.29	0.70	0.05	0.09	3.57	RGB
142	16:11:03.71	14:57:16.6	22.30	0.78	0.04	0.09	0.76	RGB
143	16:11:04.49	14:57:38.2	22.31	0.70	0.05	0.09	0.94	RGB